SUPPLEMENTARY INFORMATION

Legends for Supplementary Tables.

Supplementary Table 1. An excel file containing primary screen data. Worksheet 1, Normalized quantification data from a duplicated screen: valid data are available for 29844 unique siRNAs. **Worksheet 2**, List of 153 genes selected as candidates for positive ciliogenesis modulators. **Worksheet 3**, List of 79 genes selected as candidates for negative ciliogenesis modulators. To minimize false negative, MAX NPI and MIN NPI values from the duplicates were used for the selection of positive modulators and negative modulators, respectively.

Supplementary Table 2. An excel file containing confirmation screen data. Worksheet 1, Measurement for ciliogenesis inhibition resulted from silencing of 153 positive modulator candidates. Data (percentage of ciliated cells) was converted to Z score for plate normalization using median and MAD values from 48 non-targeting siRNAs included to each plate. Criteria for hit selection were "at least 2 siRNAs with (-) Z score $\geq$ 2.0. **Worksheet 2**, List of 40 genes selected as positive ciliogenesis modulators. Annotation of the 40 genes was obtained from ENTREZ gene database. **Worksheet 3**, Measurement for an increase in average cilium size resulted from silencing of 79 negative modulator candidates. Criteria for hit selection were "at least 2 siRNAs with Z score $\geq$ 1.2 (the variability in non-targeting controls was mainly ascribed to a decrease in cilium size; Supplementary Fig. 2b). **Worksheet 4**, List of 13 genes selected as negative ciliogenesis modulators. Annotation of the 13 genes was obtained from ENTREZ gene database.

Supplementary Table 3. An excel file summarizing hit classification study. Worksheet 1, Investigation for ciliogenesis defect caused by silencing of confirmed positive modulators using anti-acetylated tubulin immunofluorescence staining. **Worksheet 2**, Validation experiment for the result shown in worksheet 1. **Worksheet 3**, Test for serum starvation independent ciliogenesis in cells depleted with confirmed negative modulators. **Worksheet 4**, Validation experiment for the result shown in worksheet 3.

Supplementary Table 4. An excel file containing the sequences of siRNAs for selected hits.

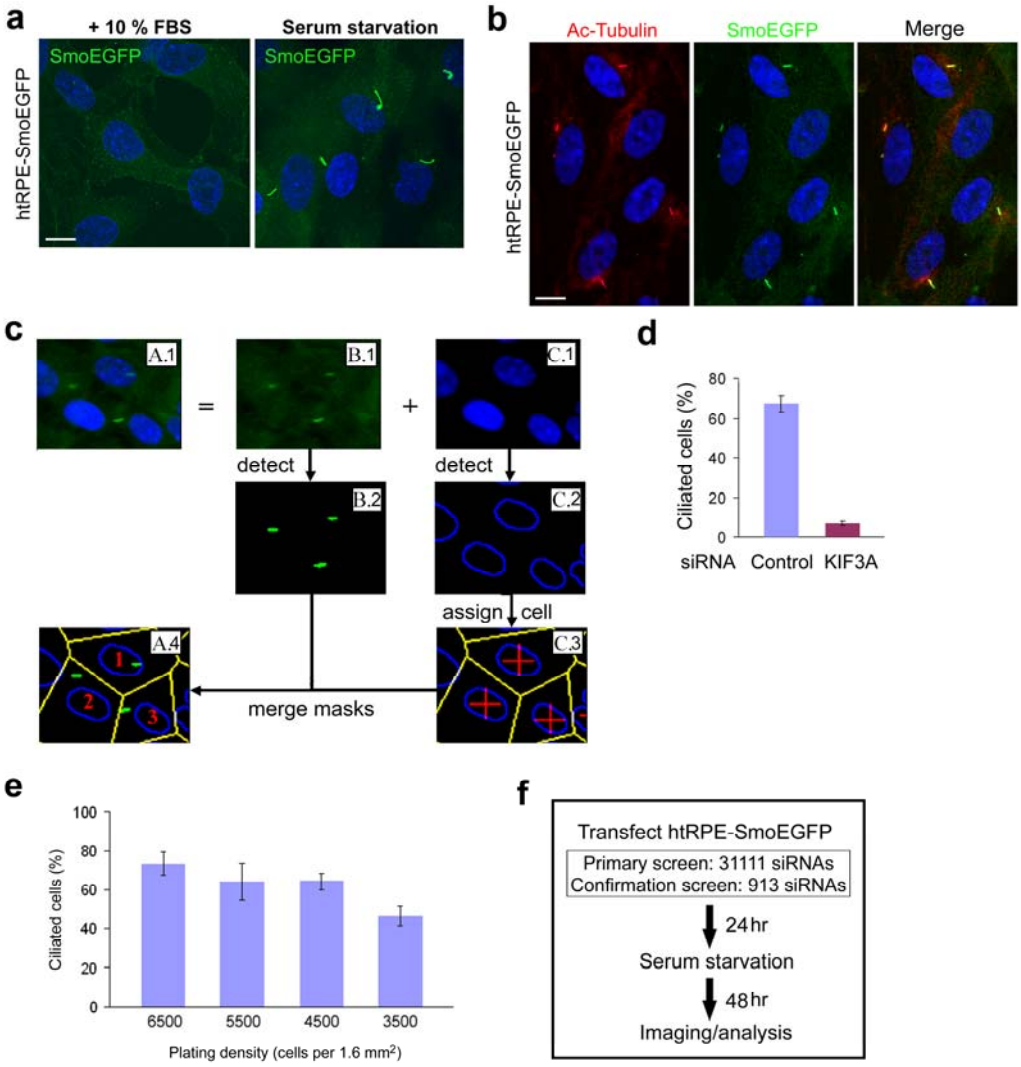

Supplementary Figure 1. Assay development. **a**, Serum starvation for 48 hrs efficiently induced ciliogenesis in htRPE-SmoEGFP cells. **b**, The specificity of SmoEGFP as a cilium maker was confirmed by co-labeling with anti-acetylated-tubulin antibody, a commonly used cilium marker. **c**, Image processing to detect cilia per cell. A.1 Merged, B.1 GFP and C.1 DAPI channel images are shown. Respective object masks for the cilia detected from the GFP image are shown in B.2 and nuclei masks detected from the DAPI image in C.2. Tessellation lines marking cell areas associated with each nucleus are shown in yellow in C.3, while nuclei outlines are shown in blue and nuclei centroids in red. A.4 shows the final segmented cell objects with nuclei outlines in blue, cell object ID in red, detected cilia in green and cell regions in yellow. **d**, Confirmation of the sensitivity of the screen strategy using a positive control siRNA. Cells were serum-starved 24 hrs after transfection and ciliated cells were counted 48 hrs later. **e**, Effect of plating density on ciliogenesis. **f**, Schematic of the primary and confirmation screen. Values, mean ± SD (n = 4 experiments). Scale bars, 10 μm.

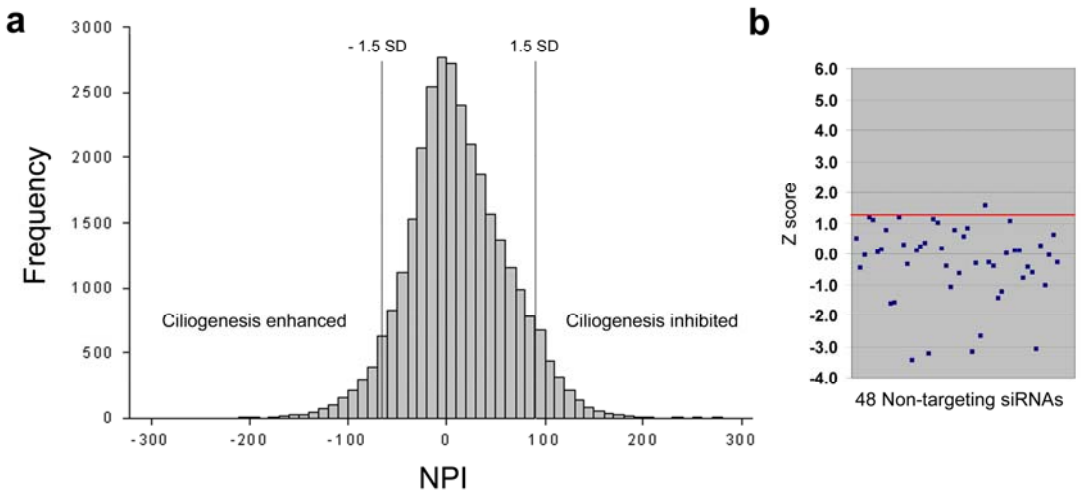

Supplementary Figure 2. Histogram and scatter plots displaying screen results. a, Histogram showing primary screen results. For normalization of plate-to-plate variability, percentages of ciliated cells were converted to normalized percent inhibition (NPI) values. Two NPI values (from duplication) for each siRNA were averaged. Overall NPI mean was 11.5, and SD was 52.0. Threshold for active siRNAs in the primary screen was set to ± 1.5 SDs. **b**, Scatter plots showing the results of cilium length measurement for 48 distinct non-targeting siRNAs tested. Only 1 non-targeting siRNA increased cilium length over Z score 1.2, indicating that cilium length increase is a highly specific phenotype.

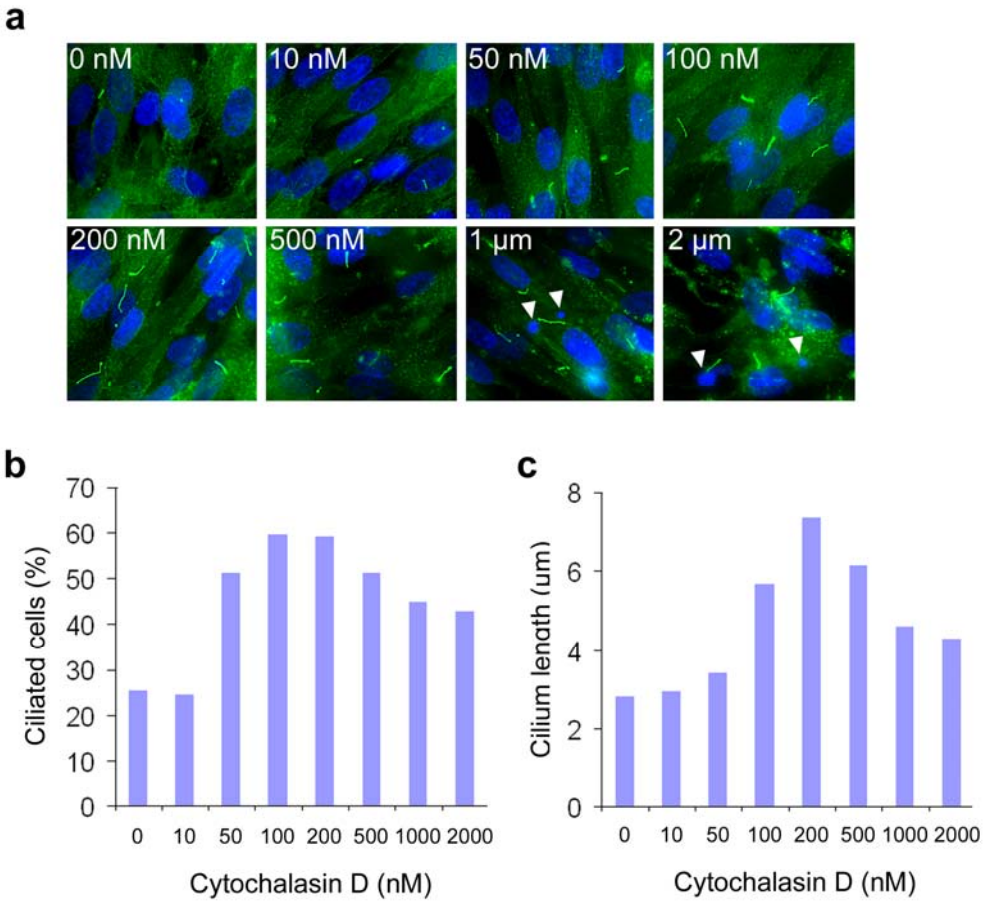

Supplementary Figure 3. CytochalasinD dose-response. a,**b**,**c**, Cells were cultured for 16 hrs in serum-free medium containing cytochalasinD. **b**, Ciliated cell numbers were increased by the treatment of cytochalasinD at 50 nM or higher. **c**, Cilium lengths were increased in cells treated with cytochalasinD at 100 nM or higher. Cell viability was affected in the presence of higher concentrations (≥ 1 uM) of cytochalasinD. Arrow, fragmented nuclei. Scale bar, 10 μm.

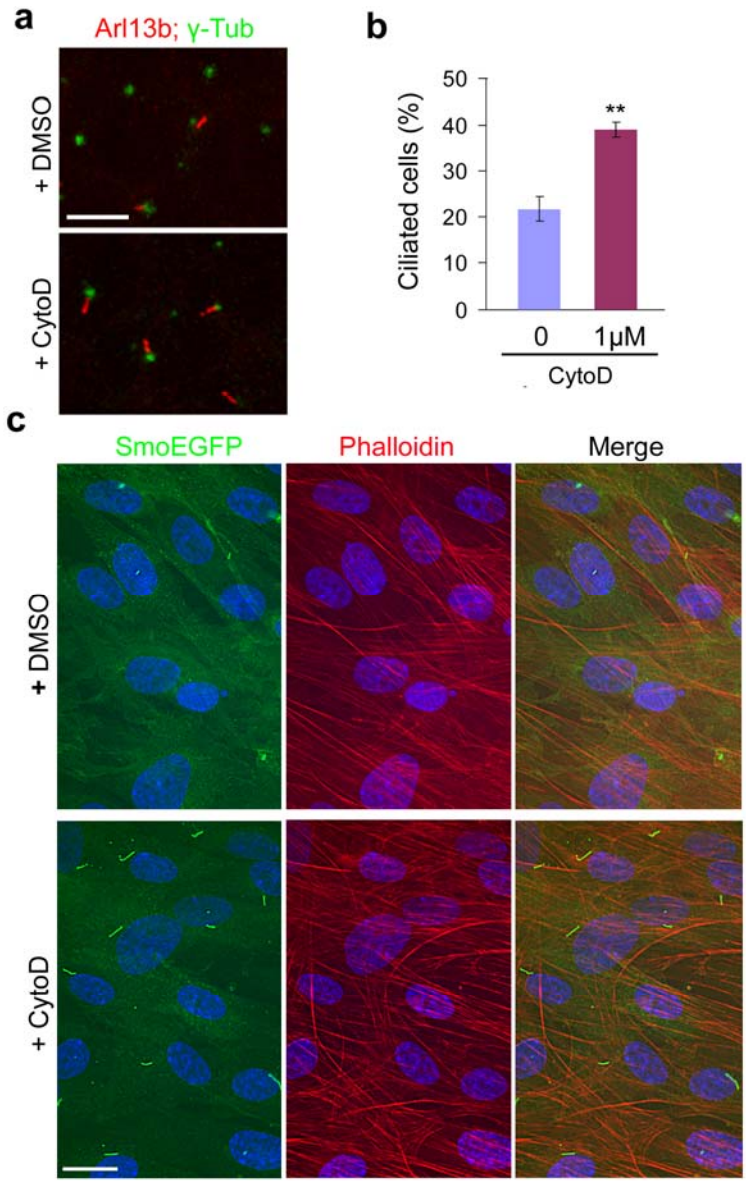

Supplementary Figure 4. CytochalasinD treatment enhances ciliogenesis without global rearrangement of actin cytoskeleton. a,b, Enhanced ciliogenesis in cytochalasinD treated HEK293T cells. HEK293T cells were serum starved for 12 hrs, and incubated for additional 12 hrs with 1 μM cytochalasinD. Cilia were labeled by Arl13b immunofluorescence (Caspary et al., 2007, Dev Cell 12:762), and the basal bodies were stained by γ-tubulin. Values, mean ± SD (n = 3 experiments). Student's t-test: **P < 0.01. **c,** htRPE cells treated with 0.5 μM cytochalasinD did not show noticeable changes in the morphology of stress fibers (labeled by phalloidin-Alexa594). Scale bars, 5 μm (a); 20 μm (c).

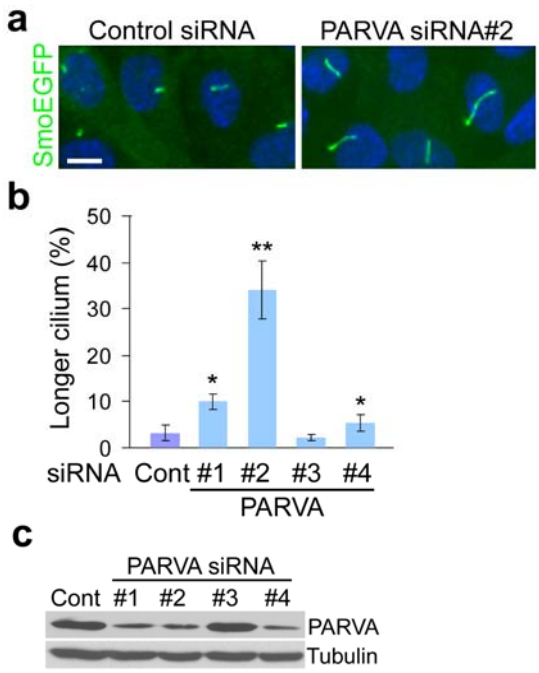

Supplementary Figure 5. PARVA is involved in negative regulation of ciliogenesis. a,**b**, PARVA knockdown significantly increased the numbers of cells with longer cilium (> 6 μm). **c**, Correlation of knockdown phenotype with protein levels was confirmed by Western blotting. Values, mean ± SD (n = 4 experiments). Student's t-test: **P* < 0.05, **P < 0.01. Scale bar, 10 μm.

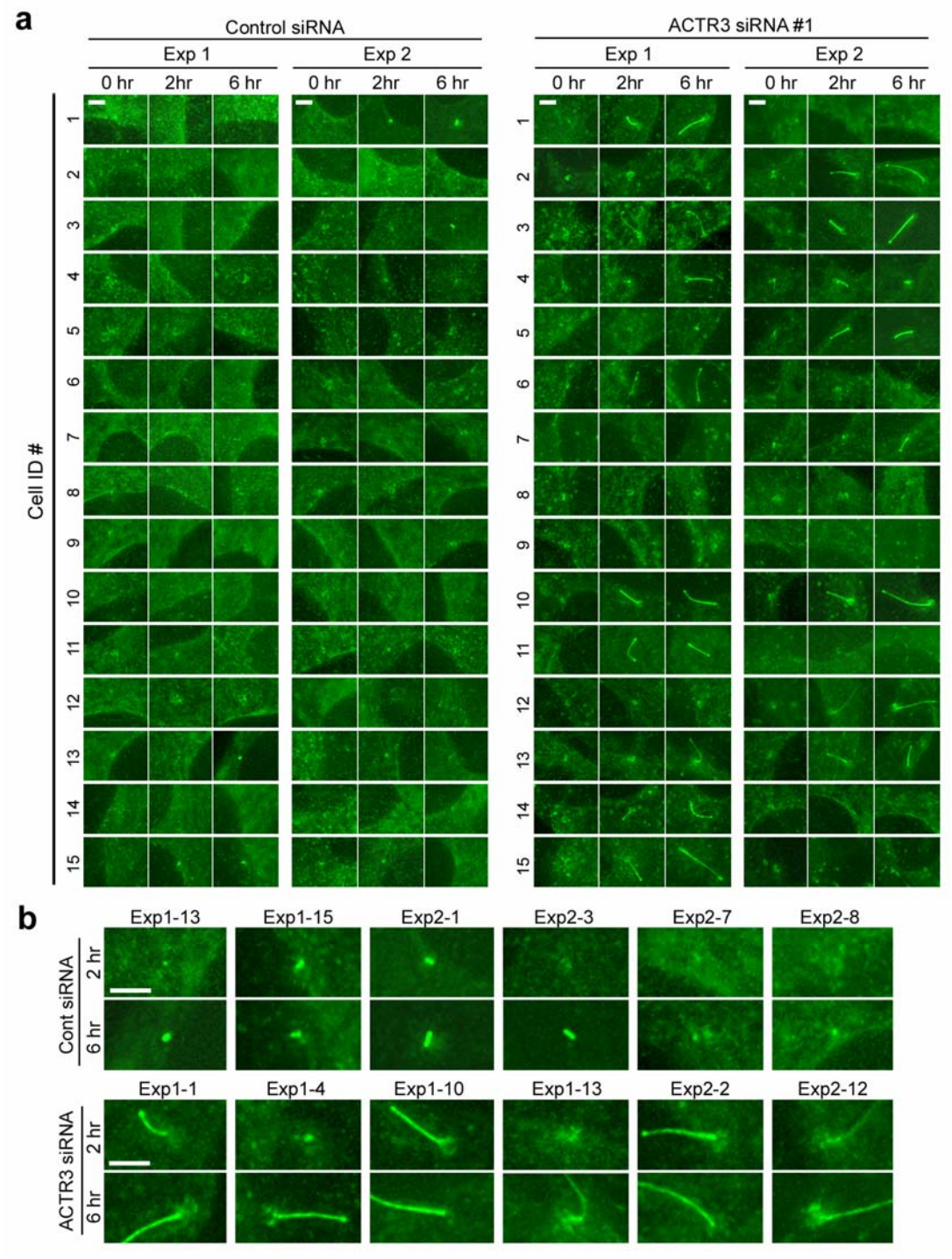

Supplementary Figure 6. Live-imaging of htRPE-SmoEGFP cells transfected with ACTR3 siRNAs. a, htRPE-SmoEGFP cells were transfected with indicated siRNAs for 2.5 days in the presence of 10 % serum and then non-ciliated cells were live-imaged for 6 hrs in serum-free medium. **b**, Magnified view of selected images. Note that cells transfected with ACTR3 siRNA#1 displayed pronounced PPC at the base of newly forming cilia. Scale bars, 2.5 μm.

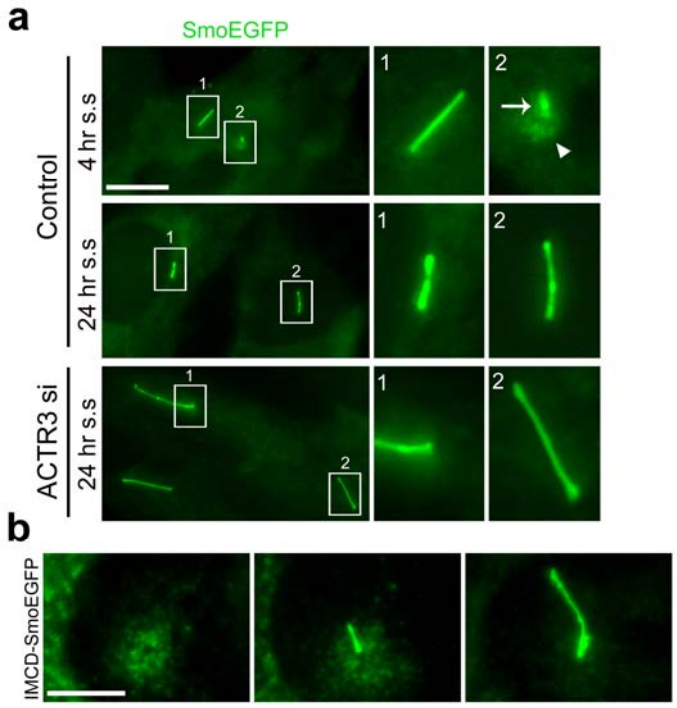

Supplementary Figure 7. PPC is a temporary structure. a, A subset of cells with premature cilia displays PPC after 4 hr serum starvation. In contrast, PPC was undetectable from most of both control and ACTR3-depleted cells with mature cilia after 24 hr serum starvation. s.s., serum starvation. Arrow, a premature cilium. Arrowhead, PPC. **b**, IMCD cells overexpressing SmoEGFP also temporarily displayed PPC at the base of nascent cilia. Scale bars, 10 μm (a); 5 μm (b).

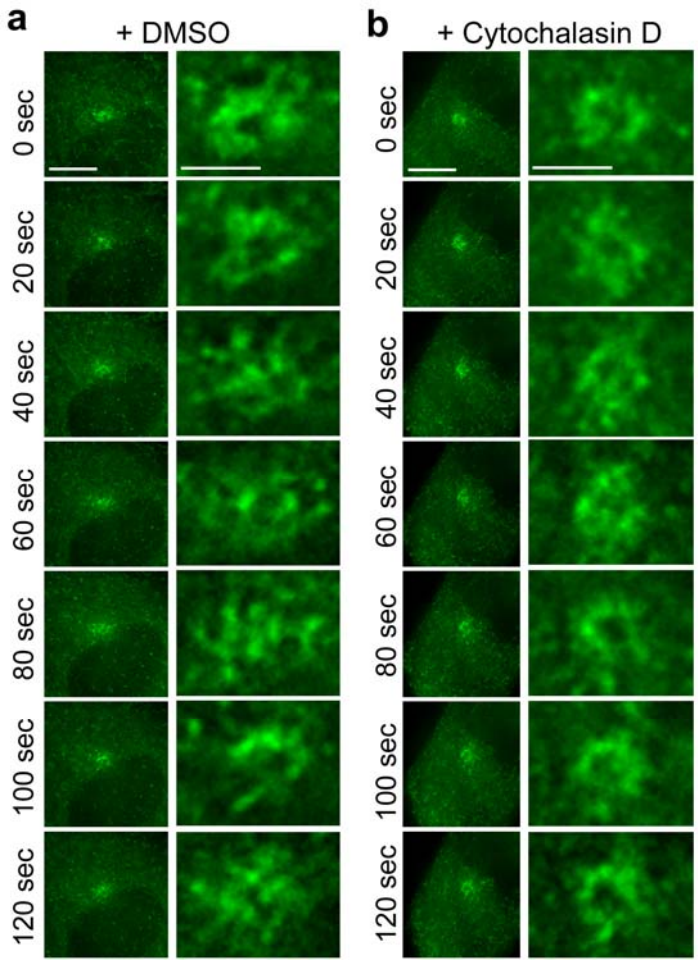

Supplementary Figure 8. CytochalasinD stabilizes PPC. a, Live imaging revealed that PPC in DMSO treated htRPE-SmoEGFP cells undergoes dynamic morphological changes. **b**, In the presence of 0.2 μM cytochalasinD, morphological changes of PPC were noticeably decreased. Right panels are magnified view of PPC. Scale bars, 10 μm (left panels); 2.5 μm (right panels).

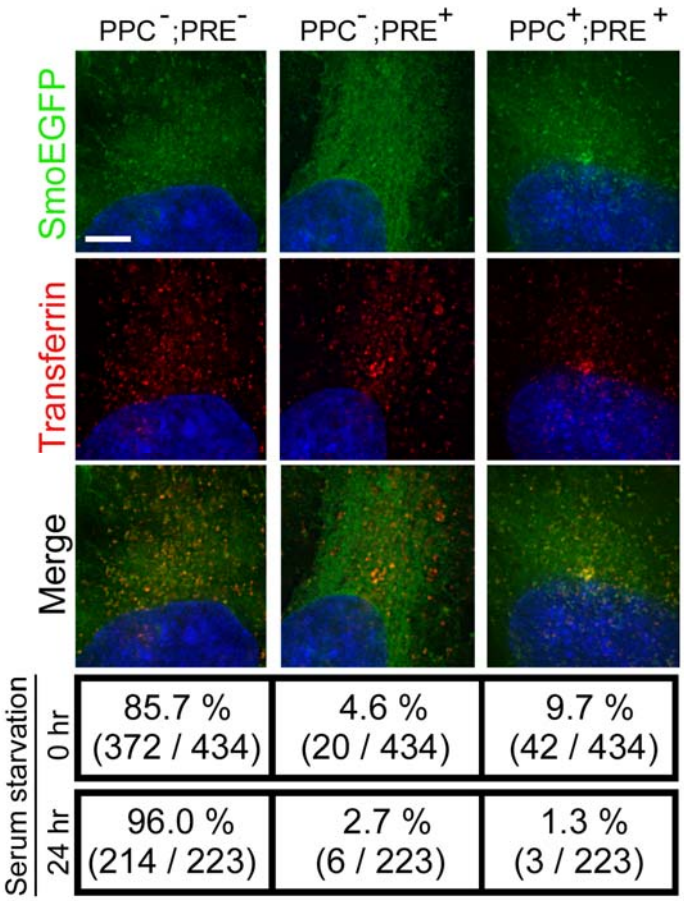

Supplementary Figure 9. PPC overlaps with pericentrosomal recycling endosomes. PPC was identified by SmoEGFP fluorescence and the pericentrosomal recycling endosome (PRE) was labeled by endocytosed transferrin-alexa594. A subset of interphase cells cultured in normal medicum (containing 10 % FBS) displayed prominent PRE. The number of cells exhibiting PRE decreased after 24 hr serum starvation. Before serum starvation, 68 % of PRE was labeled by SmoEGFP, while all SmoEGFP positive PPC was labeled by transferrin-alexa594 fluorescence, suggesting that PPC is a specific stage of PRE. Scale bar, 5 μm.

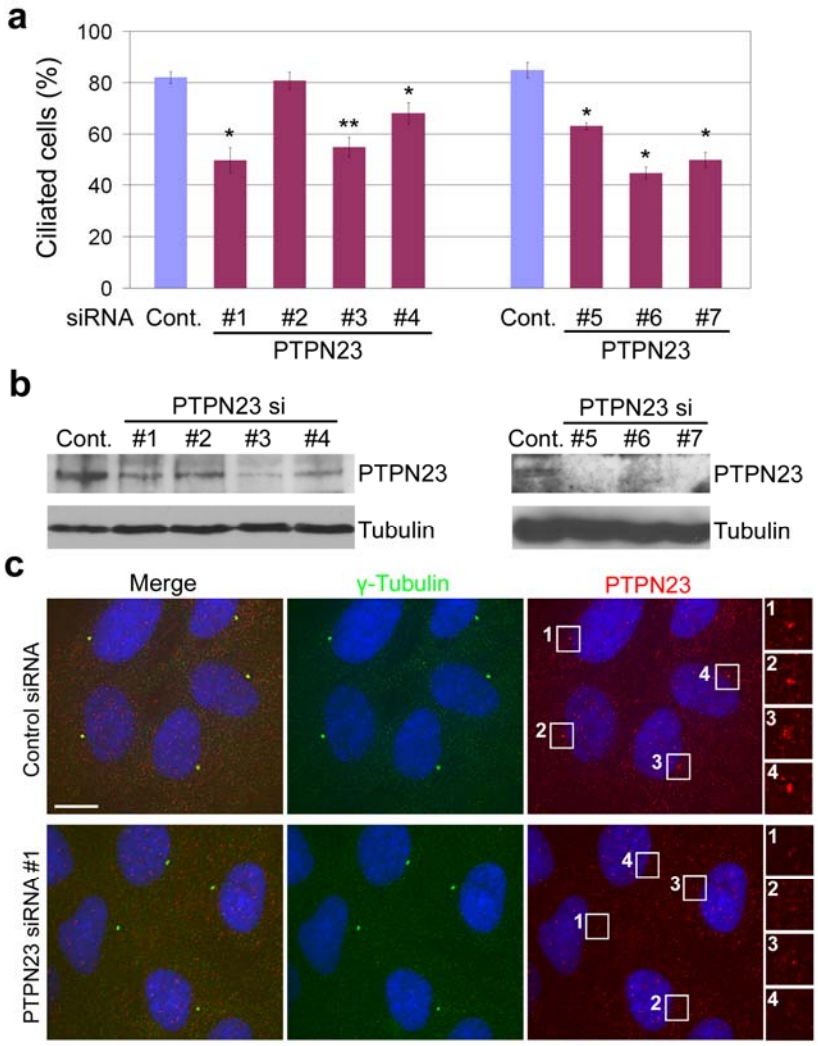

Supplementary Figure 10. Confirmation of PTPN23 knockdown phenotype. a, Multiple distinct siRNAs targeting PTPN23 significantly reduced ciliated cell numbers. Results from siRNA#1-4 are also presented in Fig. 3b. Values, mean ± SD [n = 4 (siRNA #1-4) and 2 (siRNA #5-7) experiments]. Student's t-test: $*P < 0.05$, $**P < 0.01$. **b**, Western blotting showing correlation of knockdown phenotype with protein levels. **c**, Specificity of anti-PTPN23 antibody staining was confirmed by PTPN23 knockdown. Anti-γ-tubulin antibody was used as a marker for the centrosome. Scale bar, 10 μm.

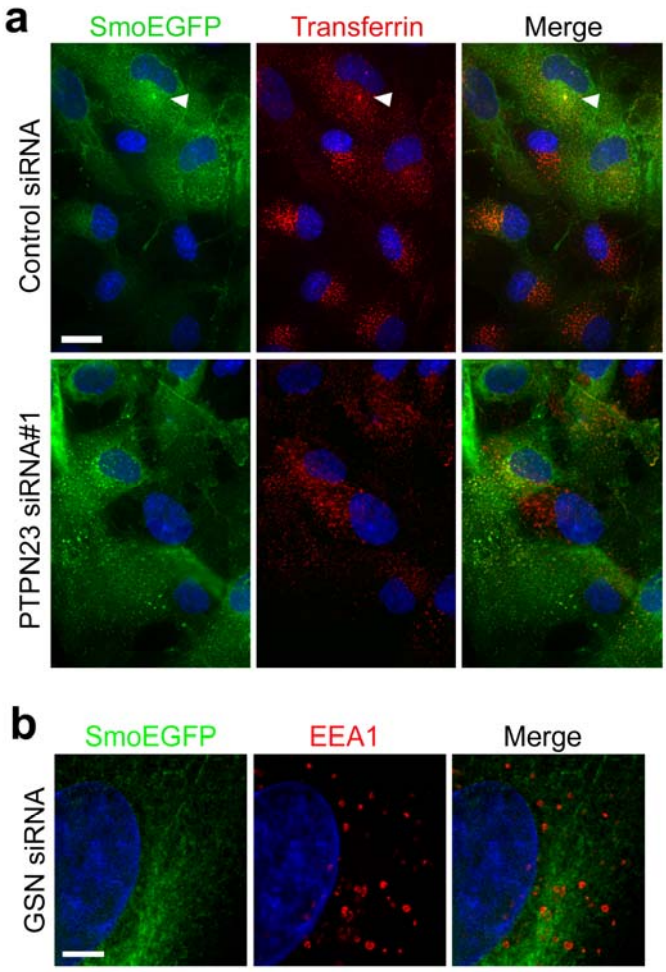

Supplementary Figure 11. PTPN23 knockdown interferes with PPC formation. a, PPC/pericentrosomal recycling endosomes (identified by SmoEGFP/endocytosed transferrin-Alexa594) were not observed in cells displaying punctuate SmoEGFP accumulation after PTPN23 knockdown. Arrow indicates cells displaying PPC/pericentrosomal recycling endosomes. **b**, In contrast to PTPN23 knockdown, GSN knockdown that inhibited ciliogenesis (Fig. 2a,b) did not cause an accumulation of SmoEGFP on EEA1 positive early endosomes. Scale bars, 20 μm (a); 5 μm(b).

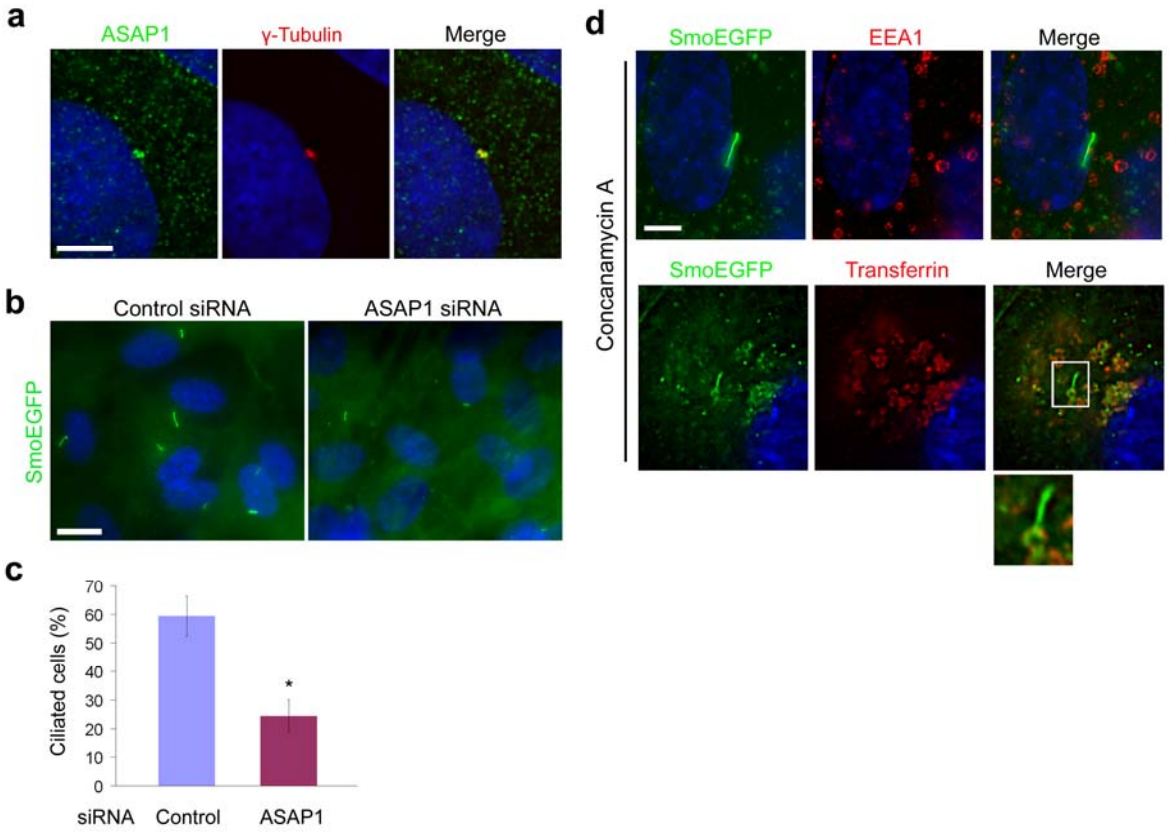

Supplementary Figure 12. Recycling route of the endocytic pathway is specifically involved in ciliogenesis. **a**, Immunofluorescence staining showing pericentrosomal enrichment of ASAP1, a component of the endocytic recycling component. **b**,**c**, ASAP1 knockdown caused a reduction of ciliated cell numbers in htRPE cells after 48 hr serum starvation. Values, mean ± SD (n = 2 experiments). Student's t-test: $*P < 0.05$. **d**, Blocking endocytic degradation pathway by concanamycinA did not cause early endosomal SmoEGFP accumulation, and did not interfere with ciliogenesis or PPC formation. Scale bars, 5 μm (a,d); 15 μm (b).

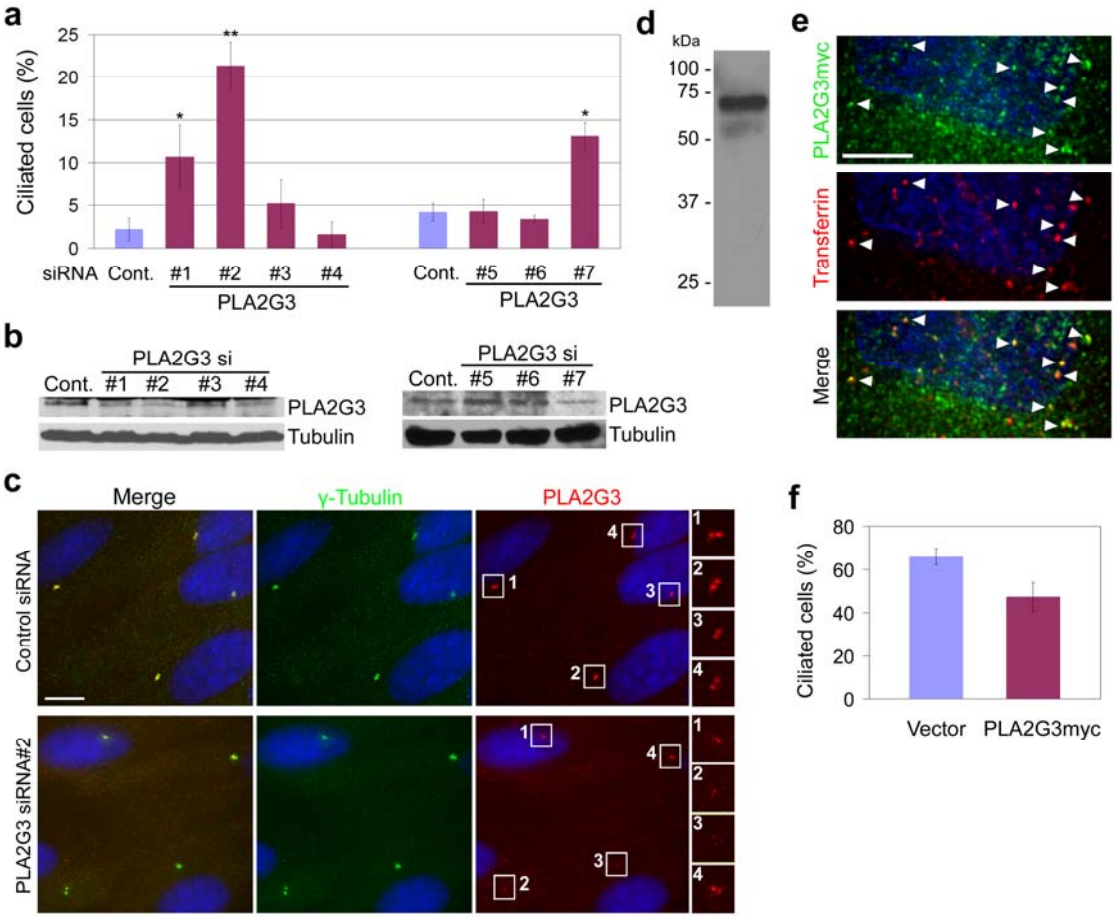

Supplementary Figure 13. Confirmation of PLA2G3 knockdown phenotype. a, Multiple distinct siRNAs targeting PLA2G3 significantly increased the number of cells with longer cilium (> 6 μm). Results from siRNA#1-4 are also presented in Fig. 3e. Values, mean ± SD [n = 4 (siRNA #1-4) and 2 (siRNA #5-7) experiments]. Student's t-test: $*P < 0.05$, $**P < 0.01$. **b**, Western blotting showing correlation of knockdown phenotype with protein levels. **c**, Specificity of anti-PLA2G3 antibody staining was confirmed by PLA2G3 knockdown. Anti-γ-tubulin antibody was used as a marker for the centrosome. **d**, Western blotting showing overexpressed full-length human PLA2G3 proteins with c-myc epitope at the C-terminus. **e**, Extensive colocalization of overexpressed PLA2G3myc and endocytosed Transferrin-Alexa594 was observed (arrows), supporting PLA2G3's involvement in the endocytic pathway. **f**, PLA2G3myc overexpression for 36 hrs in the absence of serum decreased the number of ciliated cells. Values are mean ± SD (more than 100 PLA2G3myc positive cells from two experiments were counted). Scale bars, 10 μm (c); 5 μm (e).

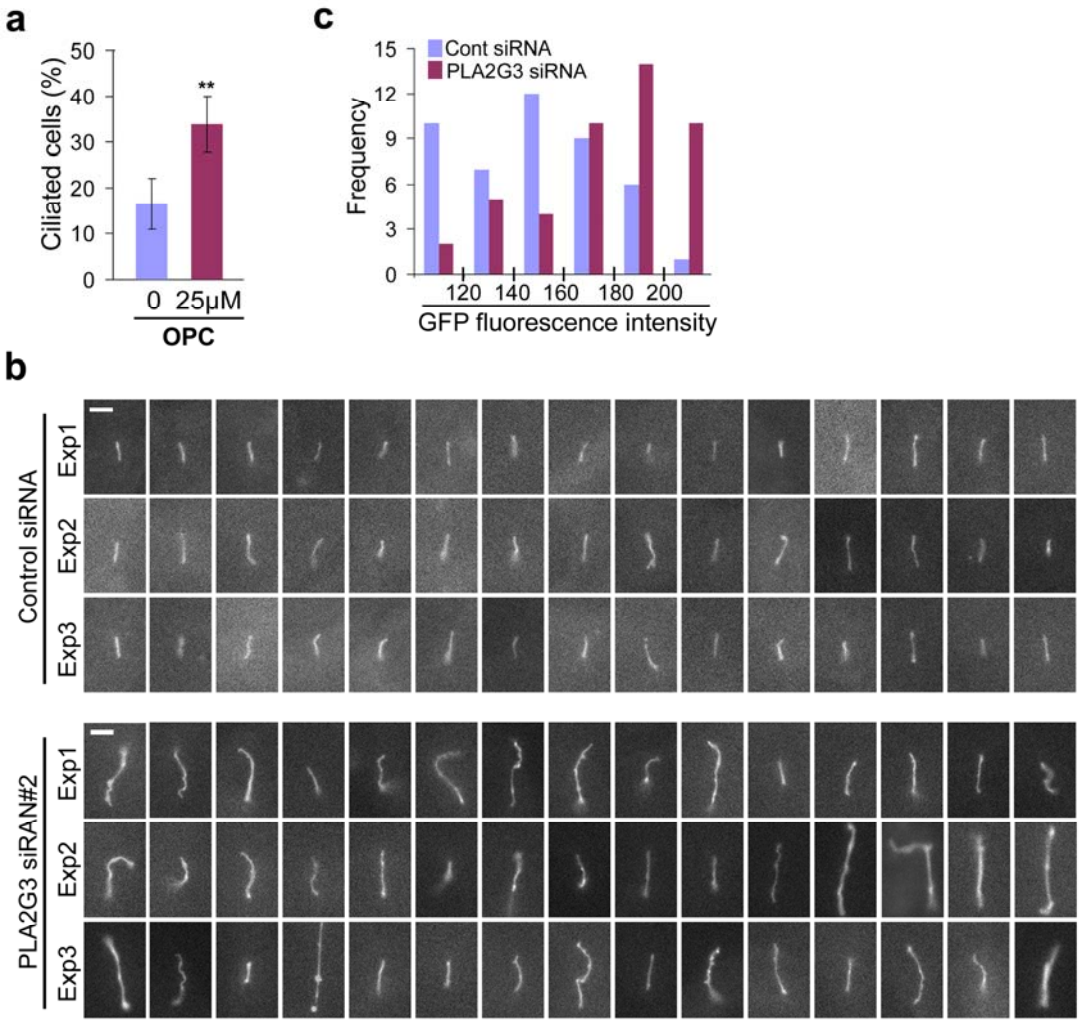

Supplementary Figure 14. Inhibition of PLA2G3 enhances ciliogenesis and ciliary SmoEGFP targeting. a, Oleyloxyethyl phosphorylcholine (OPC), an inhibitor of secreted phospholipases, caused an increase in ciliated cell number in the presence of 10 % serum. Values, mean ± SD (n = 5 experiments). Student's t-test: **P < 0.01. **b,** Images of representative ciliary EGFP fluorescence were captured 3 days after siRNA transfection (cells were cultured in serum-free medium for final 2 days). **c**, Histogram showing quantification data of the images. Fluorescent intensity is an arbitrary unit. Note that cilia from cells depleted with PLA2G3 display higher levels of SmoEGFP fluorescence. Scale bars, 2.5 μm.

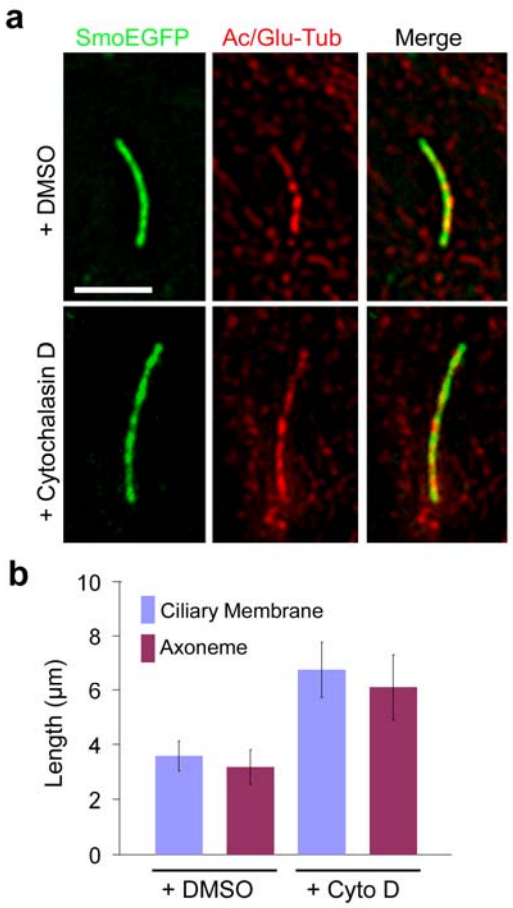

Supplementary Figure 15. CytochalasinD enhanced both axoneme assembly and ciliary membrane biogenesis. Cells were cultured in serum free medium for 24 hrs before fixation (final 16 hr with 0.2 μM cytochalasinD). **a**, Axoneme was labeled by both anti-acetylated tubulin antibody and anti-glutamylated tubulin antibody, and ciliary membrane was identified by SmoEGFP fluorescence. **b**, Quantification data of the length measurement for 25 representative cilia. Values, mean ± SD. Scale bar, 5 μm.